Available online at www.sciencedirect.com
ScienceDirect
Computational Materials Science 43 (2008) 608–615
COMPUTATIONAL MATERIALS SCIENCE
www.elsevier.com/locate/commatsci

Calculations of diffusion in FCC binary alloys using on-the-fly kinetic Monte Carlo

E.A. Bleda, Xing Gao, Murray S. Daw *

Department of Physics and Astronomy, Clemson University, Clemson, SC 29634, United States

Received 5 October 2007; accepted 7 January 2008
Available online 4 March 2008

Abstract

We present a systematic, microscopic approach to diffusion for intermetallic alloys using accelerated molecular dynamics. On-the-fly kinetic Monte Carlo is combined with an efficient saddlepoint search to find the saddlepoints exiting a valley, based on energetics from the embedded atom method. With this technique, we compute the tracer diffusivities, migration energies, short-range order and long-range order as a function of composition and temperature for examples of moderately ordered (Cu_3Au), weakly ordered (Au–Ag) and weakly clustered (Cu–Ni) alloys. We find that away from any critical temperature, the calculations produce reliable results, but when critical behavior dominates the approach is overcome by critical fluctuations.

PACS: 66.30.−h; 66.30.Pa; 66.10.cg; 66.30.Fq; 82.20.Wt

Keywords: Diffusion; Intermetallic alloys; FCC-based alloys; On-the-fly kinetic Monte Carlo; Accelerated molecular dynamics; Tracer diffusivity

1. Introduction

Diffusion in FCC-based intermetallics has been of interest for several decades. For example, it has been known for some time that the creep of structural intermetallics limits their strength at high-temperatures (see as an example the review by Miracle [1]). And yet relatively little information is available in some cases because of experimental limitations, such as a lack of a suitable isotope for tracer measurements.

Diffusion in close-packed intermetallics occurs largely vacancy-assisted under the conditions of interest. For binary alloys with some degree of ordering this represents an additionally interesting situation because of the interaction of the vacancy with its environment – as the vacancy moves it alters the ordering.

The advent of accelerated MD (AMD) techniques [2] has suggested the application of those techniques to the problem of diffusion in intermetallics. AMD is a class of techniques which intend to extend the time scale of MD-like calculations to significantly longer times through the analysis of rare events (such as diffusion). In this paper we apply a particular technique proposed by Henkelman and Jonsson [3], which they termed "on-the-fly kinetic Monte Carlo", where the possible events are continuously being explored and updated. On-the-fly kMC works well for the case of a single vacancy in somewhat disordered FCC binary alloys because the diffusion consists largely of discrete jumps from one energy valley to another, with a well-defined number (always 12 in the present application) of possible saddlepoints exiting a valley.

This approach has been tested previously on the strongly ordered Ni_3Al, with good results [4]. That particular alloy retains significant ordering all the way to the melting point. It is known also in that case that composition variation around the 3:1 stoichiometry causes significant change in the Ni-tracer diffusivity (no suitable Al tracer is available). In that work we used on-the-fly kMC to calculate the tracer diffusivities of both elements over a range of compositions

* Corresponding author.
E-mail address: daw@clemson.edu (M.S. Daw).

0927-0256/$ - see front matter © 2008 Elsevier B.V. All rights reserved.
doi:10.1016/j.commatsci.2008.01.001

near ideal stoichiometry, and demonstrated that the diffusivities are sensitive to composition. Both diffusivities showed a pronounced minimum on the Ni-rich side at 76 at.% Ni, which agrees well with experiment. The composition dependence arises from a combination of two factors: the pre-exponential of the diffusivity is increasing with increasing Ni content, and the equilibrium vacancy concentration is decreasing. The product of the two factors results in a minimum in the diffusivity on the Ni-rich side of the ideal stoichiometry.

This paper reports on the application of the same techniques to other intermetallic alloys with significantly less ordering (and including the case of weak clustering). In particular, we examine the classic case of a moderately ordered alloy (Cu_3Au), a weakly ordered example (Au–Ag), and a well-known weakly clustering alloy (Cu–Ni). For all cases, the calculations are done above the critical temperature. Our goal is to demonstrate that the technique can be used to examine the interplay between short-range ordering and diffusivity. In the latter two examples, we also vary the composition over the full range.

We find in this work that the on-the-fly kMC is well suited for calculating the tracer diffusivities in these alloys provided that critical points are avoided.

2. Method: on-the-fly kinetic Monte Carlo

Kinetic Monte Carlo has been a useful tool for decades (see, for example [5]). Where there are well-defined valleys in the energy surface separated by simple saddlepoints, the approach associates all the exits from a valley with a probability $p_i = \exp(-\Delta E_i/k_B T)$ where the ΔE_i is the energy barrier to be crossed for that exit. From that list is then selected, randomly according to the weights p_i, a single exit. That exit is taken, leading to a new valley, and the time is incremented by $dt = \tau \exp(+\Delta E_i/k_B T)$.

Kinetic Monte Carlo is usually implemented with a predefined event table. However, if the necessary saddlepoint energies cannot be categorized in a simple way, then it may become necessary to calculate saddlepoint energies on-the-fly (see, for example [3]). In the present calculation, because of the effects of temperature and stoichiometry, we are concerned with the influence of local composition on vacancy migration. We tested the dependence of vacancy migration saddlepoint energies in FCC-based alloys on the local composition near the vacancy. We found that compositional variations in the shell of fifth neighbors of the vacancy can have non-negligible effects on the saddlepoint energies. This is understandable if one considers neighbors of the atom which is exchanging with the vacancy: a second neighbor of that atom is a fifth neighbor to the vacancy. This means that in constructing a pre-defined event table, one must consider various configurations of anti-site defects out to fifth neighbors of the vacancy. The number of possible configurations in that case is quite large to be stored and re-used efficiently, making a pre-defined event table impractical.

The energetics for the kMC is obtained in this paper by the embedded aom method (EAM) [6,7], which is a semi-empirical many-atom description of metallic bonding. The EAM has been demonstrated to yield reliable results for close-packed metals and alloys. We used periodic boundary conditions, and usually used supercells of 256 atoms. The lattice constants were optimized for each composition at low temperatures. In the present calculations, we did not account for thermal expansion.

The saddlepoint search scheme has been simplified and accelerated from our earlier work [4]. Previously we had used a fairly general saddlepoint search algorithm based on the Dimer Method [8]. Because of the straightforward nature of the motion of the vacancy in an FCC binary alloy, we chose to implement a faster search algorithm more akin to the Nudged Elastic Band [9]. In the present scheme, it is straightforward to find the beginning configuration and 12 neighboring ending configurations for a vacancy hop, and then the saddlepoint is obtained by modified NEB approach.

We also keep the vacancy concentration fixed (one vacancy per cell) throughout the calculations. It is important to recall this factor because the tracer diffusivity should be proportional to the vacancy concentration, which is a function of temperature *and composition*. This must be remembered when comparing to experiment. In particular, if the assumption of single vacancy assistance holds, then the tracer diffusivity should be proportional to the vacancy concentration

$$D_A = [V] N d_A \tag{1}$$

where d_A is the result of the present calculation, N is the number of sites in our calculational cell, and [V] is the correct vacancy concentration (per site) for the given composition and temperature. The equilibrium vacancy concentration could be calculated self-consistently within our approach using equilibrium Monte Carlo.

To carry out the kMC calculations, we have written a parallel code ("pflame") tailored to a Beowulf architecture. Pflame is similar in design to the earlier Sandia Dynamo code written for vector architecture. The new implementation is written in F90, and uses straightforward MPICH communications between the processes. For the present application, we have found the most efficient strategy to be one in which the 12 saddlepoint searches are performed in parallel. All processes communicate the saddlepoint energies to the master, which picks and announces the kMC "winner", and the winning processor then broadcasts the ending configuration of its jump to all processes, and the next kMC step begins.

By comparing the initial and final configurations, we calculate the displacements of the two types and also the vacancy and from that we compute the kinetic coefficients and the corresponding tracer diffusivities. The tracer diffusion coefficient for type A in a homogeneous A–B alloy is (see [10] for a review)

$$D_A = kT\left(\frac{L_{AA}}{N_A} - \frac{L_{AB}}{N_B}\right) \quad (2)$$

where the kinetic coefficients $L_{\alpha\beta}$ are calculated from the net displacements of each type, and the N_α are the numbers of each type.

Before we run kinetic Monte Carlo, we equilibrate each configuration using eMC (equilibrium Monte Carlo) as a preparatory step. This eMC procedure consists of two mechanisms. The first mechanism involves swapping the types of two randomly chosen atoms. The second mechanism is to add a random displacement to a randomly picked atom. One of those two mechanisms is selected randomly at each step. The new configuration is either accepted or rejected according to the metropolis algorithm.

After equilibrating the configurations, we created 10 samples per temperature per concentration with one vacancy, such that the position of the vacancy is selected randomly. This approach is intended to give a better statistics. We ran kMC with 500 steps for each sample and used sub-averaging to determine statistical errors.

We also monitor the long-range order (LRO) and short-range order (SRO). The former is quickly obtained by calculating the structure factor

$$S(\vec{G}) = \sum_j \exp(i\vec{G}\cdot\vec{R}_j) \quad (3)$$

for these types of reciprocal lattice vectors: $\vec{G} = \frac{2\pi}{a}\{100\}$, $\frac{2\pi}{a}\{011\}, \frac{2\pi}{a}\{111\}$. The intensities are then used to monitor the ordering, such as tendency to $L1_2$ or $L1_0$. SRO is calculated by counting the number of nearest neighbor pairs of unlike type and comparing to what would be expected from a random occurrence at the known composition.

For the two cases where the composition was significantly varied (Au–Ag and Cu–Ni), we analyzed the calculated diffusivities over the full range of composition and temperature. We found that we could get a good representation of all the results by a simple linear variation of the migration energy with composition. To demonstrate this, we fit the results for all temperatures and compositions to a pre-exponential of the form $d(x,T) = d_0 \exp\left(-\frac{E_m(x)}{kT}\right)$, where $d(x,T)$ is the calculated tracer diffusivity as a function of composition x and T (temperature), d_0 is a constant prefactor and $E_m(x)$ is the migration energy as a function of composition. We use the *lower case d* here as a reminder that the vacancy concentration is held fixed at the same value for all compositions and temperatures. In applying the fit, we found that within the statistical uncertainties of our simulations that a linear function was sufficient to describe $E_m(x)$.

For the case of Cu_3Au, the composition was maintained at the ideal stoichiometry and the temperature was scanned from well below the critical temperature to well above. The specific results will be described in detail below, but we note here that it is not surprising to find large, in fact overwhelming, statistical variations near the critical temperature, so that our results are best for temperatures at least 20 K away from T_c.

It is best here to emphasize that our goal in the present work is the development of the parallel implementation of the on-the-fly kMC for diffusion in binary alloys, and to note that some work remains to be done to enable a complete comparison to experiment. In particular, the overall time scale τ of Monte Carlo steps is not yet determined. In the previous work [4] on Ni_3Al, the value of τ was determined by fitting to one experimental data point. It is also possible to employ a more fundamental theory, such as transition state theory [11,12], to determine τ, which would probably show some dependence on the local environment. We have left that step undone in the present case, choosing instead to emphasize the development of the parallel SP search and the extension to a wider range of materials. In addition, we also note that the vacancy concentration is fixed in these calculations, as in our previous work on Ni_3Al. In that case, because the alloy was strongly ordered and largely maintained order up to the melting temperature, we were able to apply simple arguments to obtain the point defect concentrations in the material. In the present cases where significant compositional disorder is sometimes present, we would need a more sophisticated approach, which could be afforded by an analysis of the eMC calculations, for example. In that way, it is possible to calculate the vacancy concentration predicted by the same EAM functions as a function of composition and temperature, and this step is necessary for a direct comparison to the experimental tracer diffusivities. For these two reasons, we are not yet able to make a direct comparison to experimental diffusivities, and will report on the completed work in the future. However, there are still some predictions which are independent of these considerations. For example, the ratio of the component tracer diffusivities in each binary is independent of τ and the vacancy concentration.

3. Results

3.1. Bulk tracer diffusivity for Cu–Ni

By using the technique described in the previous section, we calculated the bulk tracer diffusivity in a weakly clustered alloy, Cu–Ni. Twenty different values of Cu concentrations were picked between 5% and 90%. We excluded the extreme compositions because of poor statistics – when there are few minority atoms in the host which rely on a single vacancy for motion, there are too few events to be usable.

The temperatures were chosen in the interval 700–1300 K. Those temperatures were deliberately chosen to be well above the immiscibility temperature. Our estimate of the critical temperature for clustering – based on the equilibrium MC calculations – is well below the temperatures of the simulation. Within this temperature range, Cu–Ni remains weakly clustering. The degree of ordering was verified by calculating LRO and SRO parameters. The LRO over the range of temperatures and concentrations is negligible. However, we did observe some dependence of the weak short-range

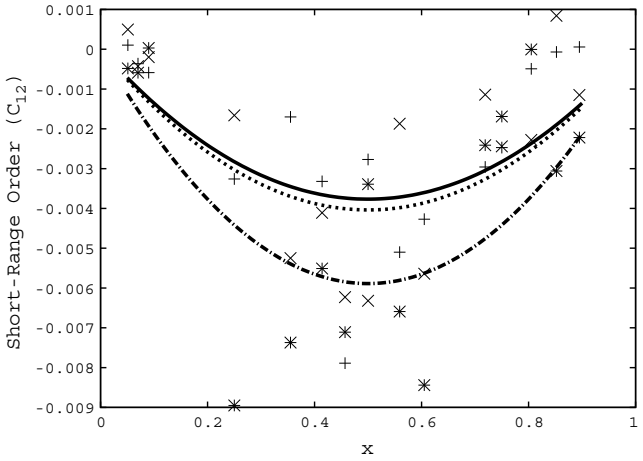

Fig. 1. Short-range order vs. Cu concentration at various temperatures in Cu–Ni. The symbols are simulation results for "+" at $T = 1300$ K, "×" at $T = 1000$ K, and "∗" at $T = 700$ K. The lines are quadratic fits for illustration – solid line at $T = 1300$ K, dashed line at $T = 1000$ K, and dot-dashed line at $T = 700$ K. C_{12} is defined as the probability of finding Cu at the vicinity of Ni relative to the probability expected for an ideal solid solution at the same concentration. The sign of the SRO indicates a tendency to cluster, as is appropriate for this alloy. The degree of SRO is small but increases some with lower temperature, as expected.

order on temperature and concentration, as is shown in Fig. 1.

In Figs. 2 and 3 we show the results for the tracer diffusivities as functions of composition at $T = 1000$ K. (We remind the reader that these results have not been corrected for the vacancy concentration, so we use the lower case d.) The statistical variability is typical for the kMC runs. The lines plotted in the figure correspond to the global fit for all compositions and temperatures, as explained next.

The complete set of calculated tracer diffusivities for Cu in Cu–Ni were fitted to the simple form $d(x,T) = d_0 \exp\left(-\frac{E_m(x)}{kT}\right)$, where $E_m(x) = xP_1 + (1-x)P_2$. The parameter P_1 is set to 0.72 eV to match the vacancy migration in pure Cu [7]. So only two parameters were used for the global fit to seven temperatures and 20 compositions. The resulting parameters are presented in Table 1. In Fig. 4 we plot in Arrhenius form the simulated diffusivities and

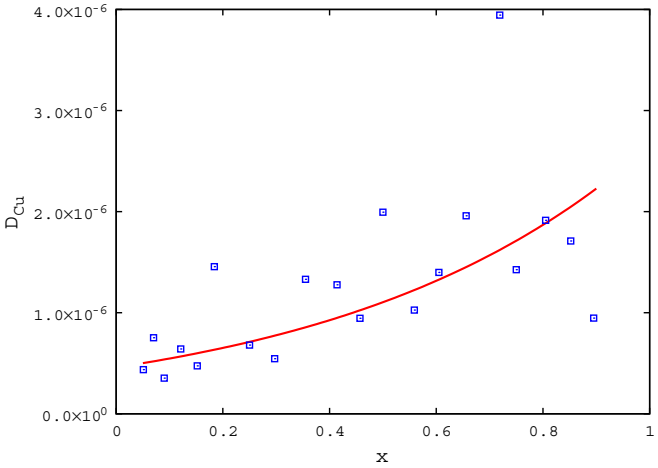

Fig. 2. Results of kMC simulations for d_{Cu} vs. Cu concentration at 1000 K. (See text for definition of the *scaled d*.) The solid is the global fit described in the text. Units of d_{Cu} are in Å^2/time, where the overall time scale is set by the kMC parameter τ.

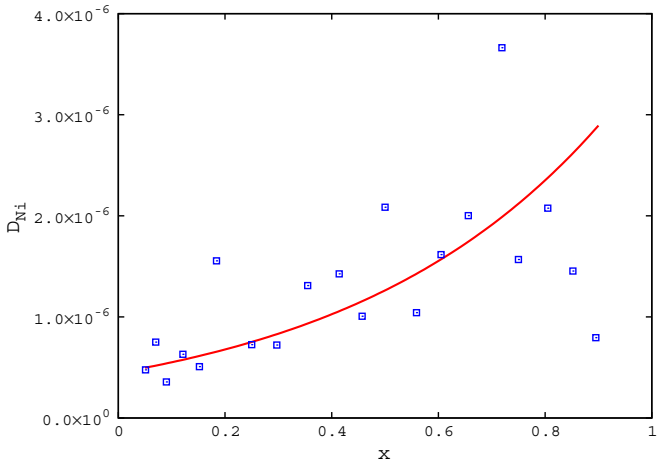

Fig. 3. Results of kMC simulations for d_{Ni} vs. Cu concentration at 1000 K. The solid is the global fit described in the text. Units of d_{Ni} are in Å^2/time, where the overall time scale is set by the kMC parameter τ. The present calculations are done at fixed vacancy concentration and must be corrected for this factor to be compared directly to experiment.

Table 1
Parameters obtained by a global fit to all of the presented kMC results for *scaled* tracer diffusivity (see text) in Cu–Ni

Type	d_0 (arb)	P_1 (eV)	P_2 (eV)
Cu	$1.13(\pm 0.08) \times 10^{-2}$	0.72	0.87 ± 0.01
Ni	$1.24(\pm 0.01) \times 10^{-1}$	0.90 ± 0.01	1.08

The functional form is described in the text. P_1 for Cu and P_2 for Ni are fixed to be consistent with vacancy migration in the pure host. The present kMC calculations of the tracer diffusivity are performed at fixed vacancy concentration, and involve an overall time factor τ which is undetermined from our simulations.

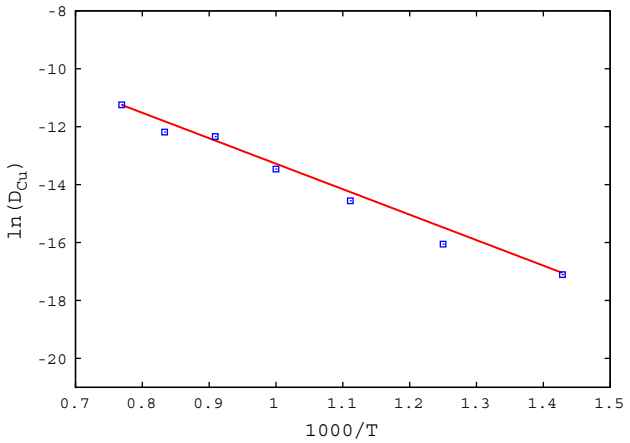

Fig. 4. Results of kMC simulations of d_{Cu} (see text) plotted in Arrhenius form at 75% Cu concentration. The solid line is the global fit described in the text. Temperatures are in K.

corresponding fit for one composition (75% Cu). The quality of the fit is comparable for other compositions.

Similarly, the complete set of calculated tracer diffusivities for Ni in Cu–Ni were fitted to the same form, but this time P_2 is set to 1.08 eV to match the result for pure Ni [7], and d_0 and P_2 are varied to obtain a global fit, which is also presented in Table 1. In Fig. 5 we plot in Arrhenius form the simulated diffusivities and corresponding fit for one composition (75% Cu). The quality of the fit is comparable for other compositions.

These calculations are of the tracer diffusivity at fixed vacancy concentration. To make a direct comparison to experiment, we must calculate the vacancy concentration as a function of composition and temperature and scale these results accordingly. Also, there is the overall kMC time scale factor (τ) which must be determined. However, ratio of the two tracer diffusivities is a prediction independent of τ and the vacancy concentration. From the fit, we predict the ratio

$$\frac{D_{\mathrm{Cu}}}{D_{\mathrm{Ni}}} = \frac{d_{\mathrm{Cu}}}{d_{\mathrm{Ni}}} = 0.091 \exp\left(+\frac{(0.21 - 0.03x)\ \mathrm{eV}}{k_{\mathrm{B}}T}\right) \quad (4)$$

which means that in the range 900–1000 K (depending on composition) the diffusivities will be about the same. At higher temperatures, $D_{\mathrm{Cu}} < D_{\mathrm{Ni}}$ and at lower temperatures the reverse will be true.

3.2. Bulk tracer diffusivity for Au–Ag

We used the same approach to examine the case of a weakly ordering alloy, Au–Ag. We chose nine compositions from the range 10–90% and temperatures from the range of 800–1300 K. Again, the temperatures are well above the ordering temperature – either the experimental or our calculated values. Our equilibrium MC calculations show negligible long-range order, and some weak short-range ordering which depended on composition and temperature, as shown in Fig. 6.

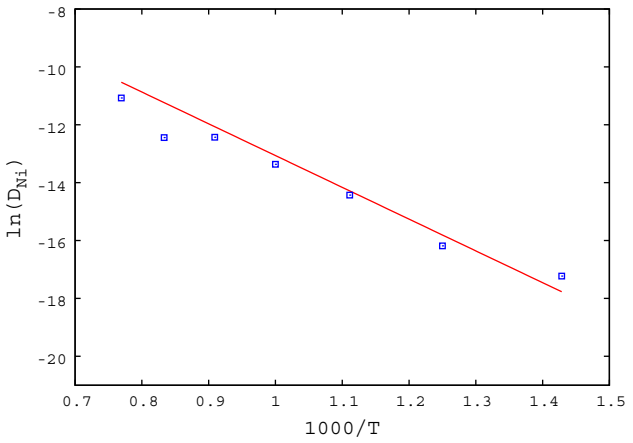

Fig. 5. Results of kMC simulations of d_{Ni} (see text) plotted in Arrhenius form at 75% Cu concentration. The solid line is the global fit described in the text. Temperatures are in K.

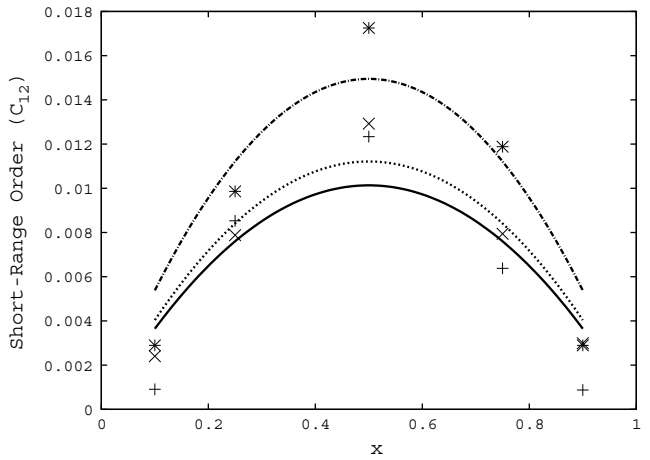

Fig. 6. Short-range order vs. Ag concentration at various temperatures in Au–Ag. The symbols are simulation results for "+" at $T = 1000$ K, "×" at $T = 800$ K, and "∗" at $T = 600$ K. The lines are quadratic fits for illustration – solid line at $T = 1000$ K, dashed line at $T = 800$ K, and dot-dashed line at $T = 600$ K. C_{12} is defined as the probability of finding Au at the vicinity of Ag relative to the probability expected for an ideal solid solution at the same concentration. The sign of the SRO indicates a tendency to order, as is appropriate for this alloy. The degree of SRO is small but increases some with lower temperature, as expected.

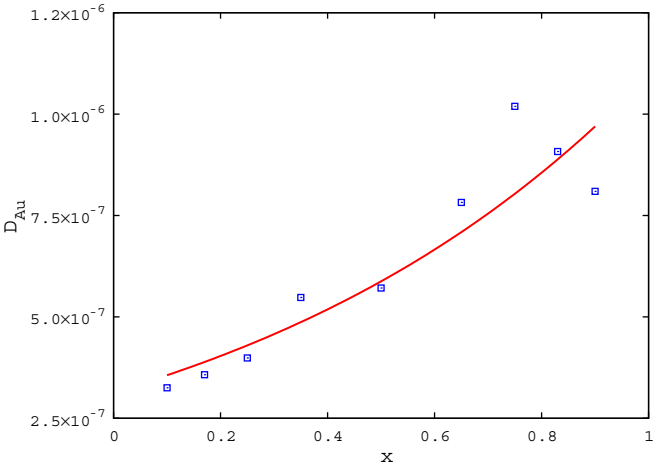

Fig. 7. Results of kMC simulations for d_{Au} vs. Au concentration at 800K. The solid is the global fit described in the text. Units of d_{Au} are in Å^2/time, where the overall time is set by the kMC parameter τ.

In Figs. 7 and 8 we show the results for the tracer diffusivities as functions of composition at $T = 800$ K. The statistical variability is typical for the kMC runs. The lines plotted in the figure correspond to the global fit for all compositions and temperatures, as will be explained next.

The complete set of calculated tracer diffusivities for Au in Au–Ag were fitted to the simple form $d(x,T) = d_0 \exp(-\frac{E_{\mathrm{m}}(x)}{kT})$, where $E_{\mathrm{m}}(x) = xP_1 + (1-x)P_2$. The parameter P_1 is set to 0.71 eV to match the vacancy migration in pure Au [7]. So only two parameters were used for the global fit to six temperatures and nine compositions. The resulting parameters are presented in Table 2. In Fig. 9 we plot in Arrhenius form the simulated diffusivities and

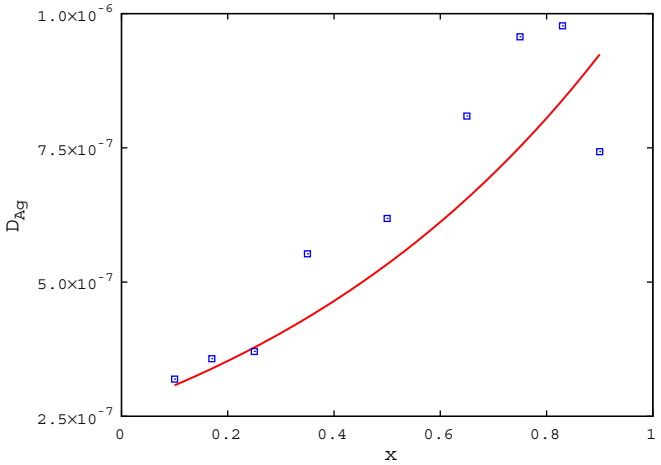

Fig. 8. Results of kMC simulations for d_{Ag} vs. Au concentration at 800 K. The solid is the global fit described in the text. Units of d_{Ag} are in Å^2/time, where the overall time is set by the kMC parameter τ.

Table 2
Parameters obtained by a global fit to all of the presented kMC results for *scaled* tracer diffusivity (see text) in Au–Ag

Type	d_0 (arb)	P_1 (eV)	P_2 (eV)
Au	$3.23(\pm 0.00) \times 10^{-2}$	0.71	0.80 ± 0.01
Ag	$4.54(\pm 0.00) \times 10^{-2}$	0.74 ± 0.01	0.83

The functional form is described in the text. P_1 for Au and P_2 for Ag are fixed to be consistent with vacancy migration in the pure host. The present kMC calculations of the tracer diffusivity are performed at fixed vacancy concentration, and involve an overall time factor τ which is undetermined from our simulations.

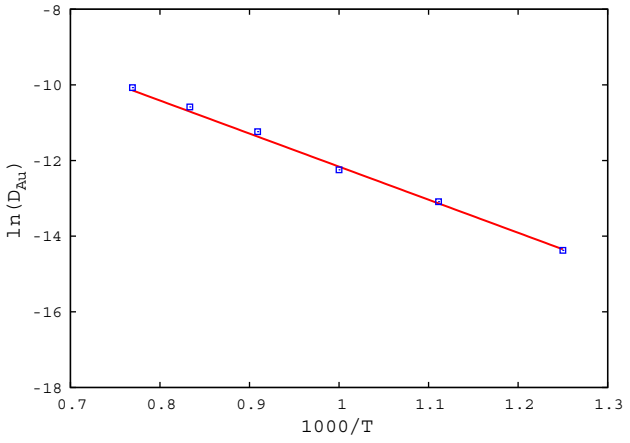

Fig. 9. Results of kMC simulations of d_{Au} plotted in Arrhenius form at 50% Au concentration. The solid line is the global fit described in the text. Temperature is in K.

corresponding fit for one composition (50% Au). The quality of the fit is comparable for other compositions.

Similarly, the complete set of calculated tracer diffusivities for Ag in Au–Ag were fitted to the same form, but this time P_2 is set to 0.83 eV to match the result for pure Ag [7], and d_0 and P_1 are varied to obtain a global fit, and the results are also presented in Table 2. In Fig. 10 we plot in Arrhenius form the simulated diffusivities and corresponding fit for one composition (50% Au). The quality of the fit is comparable for other compositions.

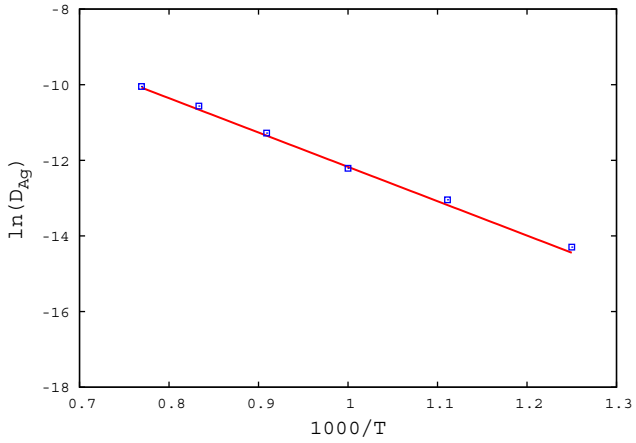

Fig. 10. Results of kMC simulations of d_{Ag} plotted in Arrhenius form at 50% Au concentration. The solid line is the global fit described in the text. Temperature is in K.

As for the Cu–Ni calculations, these calculations for Au–Ag are at fixed vacancy concentration, and involve an (as yet) undetermined kMC time scale factor τ. The ratio of the two tracer diffusivities is a prediction independent of these factors. From the fit, we predict the ratio

$$\frac{D_{Au}}{D_{Ag}} = \frac{d_{Au}}{d_{Ag}} = 0.711 \exp\left(+\frac{0.03\ \text{eV}}{k_B T}\right) \tag{5}$$

which means that in the range of the temperatures considered here (800–1300 K) we have $D_{Au} \approx D_{Ag}$.

3.3. Bulk tracer diffusivity for Cu_3Au

Turning now to the ordered Cu_3Au alloy, we performed the same on-the-fly kMC calculation of tracer diffusivities but only for the stoichiometric composition. The cells were slightly larger for these calculations (864 atoms), and the temperature range (200–1200 K) includes the calculated order–disorder transition – which occurs at around 300 K for these functions.

The results of the eMC anneal are illustrated in Fig. 11, which shows the calculated LRO and SRO parameters as functions of temperature for Cu_3Au. The sharpness of the transition as expressed in the LRO parameter, along with some degree of statistical variability, is to be expected for the finite size of the cell and number of eMC steps. The figure also shows that significant short-range ordering persists well above the transition, indicating that this is a case where the ideal solid solution would be a poor description. For example, the calculated SRO at 500–600 K (about twice the critical temperature) indicates that the composition of the averaged local environment is about half way between solid solution and $L1_2$.

In Fig. 12 we show the calculated values of d_{Au} and d_{Cu} above the critical temperature, plotted in an Arrhenius form. The high-temperature data are fitted to a strict

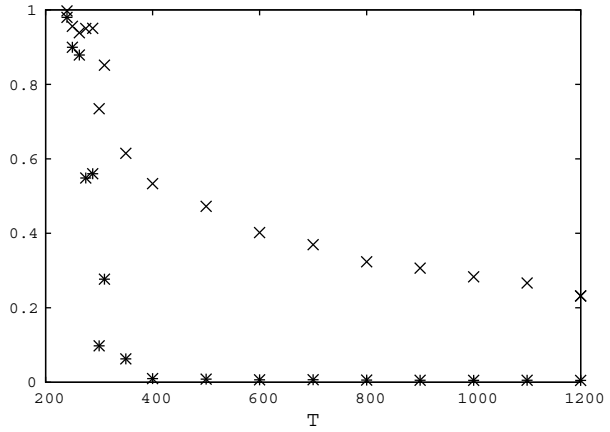

Fig. 11. Long-range and short-range order parameters for Cu_3Au, according to the equilibrium MC calculations presented here, as a function of temperature (K). Both LRO ("plus–×" symbol) and SRO ("×" symbol) are scaled to be unity in the low temperature ($L1_2$) phase and to vanish for ideal solid solution. The calculated critical temperature is about 290 K. Significant SRO persists well above the critical temperature.

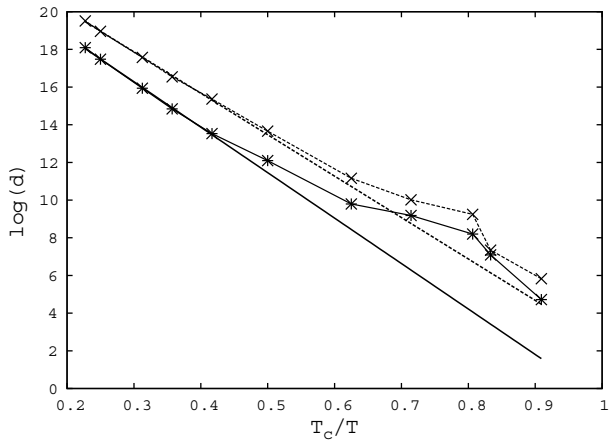

Fig. 12. Arrhenius plot of the calculated *scaled* tracer diffusivities (see text) for Cu_3Au above the critical temperature. The "×" symbols are for Au and "plus–×" for Cu. The lines are Arrhenius fits to the high-temperature data. Significant deviation from strict Arrhenius behavior occurs below a temperature of $2T_c$.

Arrhenius form and that fit is shown a straight lines for comparison. The ratio $D_{Au}/D_{Cu} = d_{Au}/d_{Cu}$ is in the range of 2–6 over the entire plot. The figure also shows that the diffusivities are Arrhenius at high temperature but deviate significantly as the temperature is cooled to the transition. A comparison between this figure and the previous one (Fig. 11) would suggest a relationship between the local ordering and the tracer diffusion, as would be expected. We leave the discussion of this relationship to the next section. We note that for temperatures within 20% of the transition that there is a significant increase in the statistical variations, which is consistent with the known critical behavior of order–disorder systems near the transition. Near the critical temperature, increasingly large fluctuations in the ordering occur and are visible even in the small supercells used here, and these are reflected in the larger statistical variations present at the lower temperatures.

We have also calculated the tracer diffusivities below the transition, and find a situation similar to the stoichiometric results for Ni_3Al using a similar method [4]. The majority species Cu is much more mobile than the minority Au even up to within 10% of the transition temperature, and the diffusivity appears to be ideally Arrhenius. We also note, as in the previous work, that the calculations become increasingly inefficient at these low temperatures because of the tendency of the vacancy to bind to configurational defects.

4. Discussion

The results of this paper demonstrate that the on-the-fly kMC method is sufficiently robust to provide reasonable results for the tracer diffusivities in binary intermetallic alloys showing significant deviations from ideal solid solution. In combination with a previous publication, we have considered a wide range of behavior, from strongly ordered (Ni_3Al), moderately ordered (Cu_3Au), weakly ordered (Au–Ag), and weakly clustered (Cu–Ni). The limitation of this local method is clearly present near critical transitions, where large fluctuations in the local environment become statistically overwhelming. We also find that at low temperatures in the ordered phase that the vacancy can spend a large number of steps moving locally without accomplishing significant displacements or accumulating much simulated time. For these reasons, a more strategic method would be required to treat the entire range of temperatures and compositions, but this method does provide useful results.

In particular, we see in the present results for the moderately ordered alloy (Cu_3Au) significant deviation from Arrhenius behavior as the temperature is lowered from above the critical temperature. Not surprisingly, there is correlation with the SRO parameter in this case. We prefer here to express this correlation differently, by looking at the composition of the environment of the vacancy, which we do now.

In the two examples which approach ideal solid solution – (Cu–Ni) and Au–Ag – a quick calculation shows a weak binding of the vacancy to compositional variations. For example, in a Au host, the vacancy is weakly repelled (by 0.03 eV) by a Cu impurity. Similarly, for the other combinations, (Au in Cu, Ag in Au, Au in Ag), the interactions are all less than 0.03 eV in magnitude. However, in a Cu host, a vacancy is relatively strongly bound (by 0.14 eV) to a Au impurity. We also find that the vacancy attracts Au neighbors in the Cu_3Au alloy above the critical temperature. For example, our eMC calculations show that a vacancy manages to have 4.2 Au nearest neighbors (of 12 possible) on average at 600 K, increasing to 5.0 at 400 K. We emphasize that our kMC calculations use the same EAM functions and therefore encapsulate these same energetics, which are incorporated in the calculation of tracer diffusivities.

We conclude then by anticipating further analysis of the tracer diffusion in intermetallic alloys using on-the-fly kinetic Monte Carlo. We have demonstrated here that this technique is especially useful at higher temperatures over a wide range of compositions.

Acknowledgement

The authors acknowledge the support from NSF-ITR.

References

[1] D. Miracle, Acta Metall. Mater. 41 (1993) 649.
[2] A.F. Voter, F. Montalenti, T.C. Germann, Ann. Rev. Mater. Res. 32 (2002) 321.
[3] G. Henkelman, H. Jonsson, J. Chem. Phys. 115 (2001) 9657.
[4] C. Harris, R. Tedstrom, M.S. Daw, M.J. Mills, Comput. Mater. Sci. 37 (2006) 462.
[5] K.A. Fichthorn, W.H. Weinberg, J. Chem. Phys. 95 (1991) 1090.
[6] M.S. Daw, S.M. Foiles, M.I. Baskes, Mater. Sci. Rep. 9 (1993) 251.
[7] S.M. Foiles, M.I. Baskes, M.S. Daw, Phys. Rev. 33 (1986) 7983.
[8] G. Henkelman, H. Jonsson, J. Chem. Phys. 111 (1999) 7010.
[9] G. Henkelman, H. Jonsson, J. Chem. Phys. 113 (2000) 9978.
[10] R.E. Howard, A.B. Lidiard, Rep. Prog. Phys. 27 (1) (1964) 161.
[11] D. Chandler, J. Chem. Phys. 68 (1978) 2959.
[12] J.A. Montgomery, D. Chandler, B.J. Berne, J. Chem. Phys. 70 (1979) 4056.